energies

Article

Airtightness Assessment under Several Low-Pressure Differences in Non-Residential Buildings

Chanhyung Shim and Goopyo Hong *

Department of Architectural Engineering, College of Engineering, Kangwon National University, Samcheok 25913, Republic of Korea; sim9710@kangwon.ac.kr
* Correspondence: goopyoh@kangwon.ac.kr

Abstract: The thermal performance of building envelopes is significantly affected by building insulation and airtightness. However, most studies have focused on improving thermal performance in building envelopes, while few studies on improving airtightness in buildings have been conducted. The present study measured airtightness and infiltration in non-residential buildings using fan pressurization and tracer gas methods. By analyzing the results obtained from both methods, the distribution of the correlation factors was identified, which can be used for the air leakage rates obtained from the blower door test to estimate the infiltration rates under natural airflow conditions. Since it is difficult to get the values of ACH50 through the blower door test in buildings of large volume or where large air leakages occur, the study proposed a method to convert the values of airtightness under several low-pressure differences of 20 Pa, 25 Pa, 30 Pa and 35 Pa into ACH50 using conversion coefficient. By dividing the air leakage rate under 20 Pa pressure difference by the conversion coefficient of 0.60, the values of ACH50 can be estimated. Results converted to ACH50 using conversion coefficient for various pressure differences of 20 Pa, 25 Pa, 30 Pa, and 35 Pa showed an error of 0.1–4.4%, respectively, compared to actual ACH50 measurement results.

Keywords: airtightness; blower door; ACH50; non-residential building

Citation: Shim, C.; Hong, G. Airtightness Assessment under Several Low-Pressure Differences in Non-Residential Buildings. *Energies* **2023**, *16*, 6845. https://doi.org/10.3390/en16196845

Academic Editors: Miroslava Kavgic and Abdulhameed Babatunde Owolabi

Received: 31 August 2023
Revised: 18 September 2023
Accepted: 22 September 2023
Published: 27 September 2023

1. Introduction

1.1. Background and Objective

With the significant concern for climate change in response to global warming, the Intergovernmental Panel on Climate Change (IPCC) has agreed to achieve the goal of net zero by 2050 to limit temperature increase to 1.5 °C by 2100. Thus, many countries have agreed to reduce greenhouse gas (GHG) emission rates [1]. The building sector in the EU accounts for about 40% of total energy consumption [2–4]. In addition, 60–70% of building energy consumption was used for space heating. Among possible strategies to reduce building energy consumption, one of the most effective strategies is to improve the thermal performance of building envelope systems [5]. In residential buildings, the exterior walls contributed about 34% of building energy consumption, which was important in determining the energy demand for indoor thermal comfort [5,6].

In the Energy Conservation Design Standard of buildings in Republic of Korea, the government has strengthened the thermal properties of building envelopes by about 15–20% every two or three years since 2008 [7]. Specifically, the thermal transmittance value from 2008 to 2022 was changed from 0.47 W/m^{2}K to 0.15 W/m^{2}K, respectively. This shows an approximate decrease in thermal transmittance of 70%. Even though building insulation and airtightness are both important for the thermal properties of building envelopes, the Korean government has only focused on building insulation performance. In addition, there have been a few studies of the infiltration in building energy consumption [8]. In the total heat loss of buildings, infiltration accounted for about 15–60%.

Moreover, air leakage has demanded about 25% and 12% of heating and cooling, respectively [9]. The improvement of airtightness in buildings can be considered an effective way to minimize heat loss. In the case of high-performance buildings, the effectiveness of the improved airtightness can be relatively greater [10,11].

Generally, airtightness can play a significant role in building energy efficiency [11–15]. Recently, much attention has been paid to the importance of building airtightness [15–17]. Exfiltration is estimated to account for 3–5% and 11–15% of the total energy demand and CO_2 emissions in UK housing stock, respectively [1]. Thus, improving airtightness in building envelopes is necessary, which can result in improved building energy efficiency and indoor air quality [18,19].

To assess building airtightness, two methods have been commonly used: the fan pressurization method and the tracer gas method [20–22]. The fan pressurization method measures the airflow at an artificial condition of 50 Pa or 10 Pa of pressure difference between indoors and outdoors. In addition, the air leakage rates from the measurement can be used as a metric for the air leakage rates on the unit area of the building envelope [23–25]. The airtightness value in natural conditions is quite a bit lower than that under a 50 Pa pressure difference between indoors and outdoors. Specifically, the pressure difference between indoors and outdoors under the natural airflow condition is lower than 10 Pa [26]. Generally, the tracer gas method has been used to measure infiltration under natural air flow conditions, and it can provide a more reliable result than that offered by the fan pressurization method [27–29].

For the objectives of the present study, the infiltration rates for non-residential buildings were regularly measured using the tracer gas method and the fan pressurization method to identify the correlation factor. The measurements assessed the airtightness of non-residential buildings, and the correlation factor was recognized by the analyses of the results obtained from the two methods. Since it is difficult to maintain a 50 Pa pressure difference for the blower door test in buildings of large building volume or which are old, the present study also proposed a method to convert the values of airtightness under several low-pressure differences of 20 Pa, 25 Pa, 30 Pa and 35 Pa into ACH_{50}. The overall flow of this study is displayed in Figure 1.

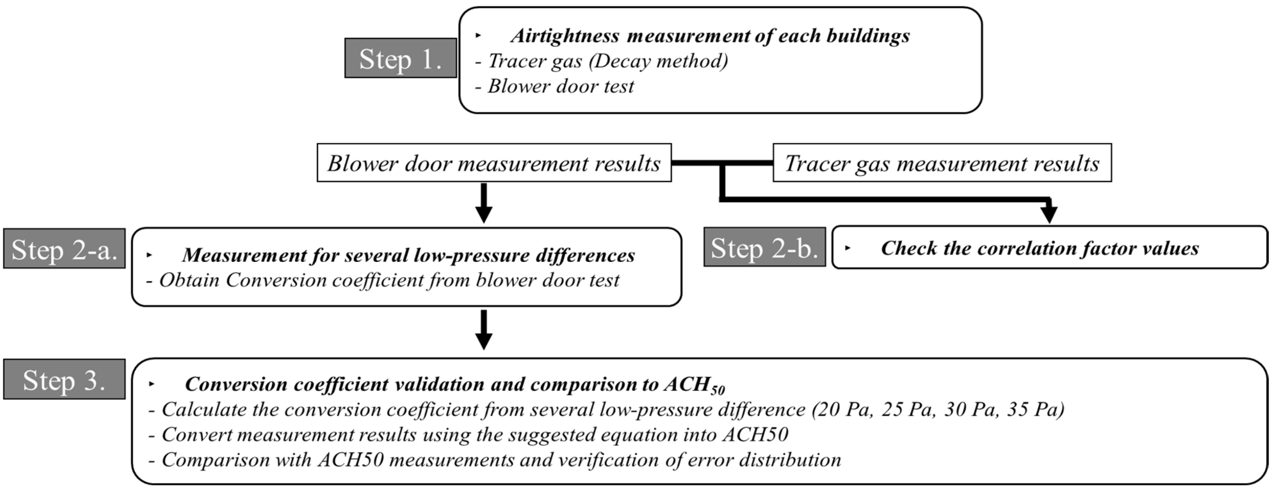

Figure 1. Research Framework.

1.2. Literature Review

Sherman proposed a simple rule-of-thumb of the "air changes per hour under 50 Pa" (hereafter ACH_{50}/N (N = the correlation factor, 20), divided-by-20 rule) [30,31] and correlation factor simply consists of the assumption that the infiltration in a building is 1/20th of its airtightness [32]. However, recent studies have revealed that the correlation factor can differ by building location and climate conditions and that a correlation factor greater than 20 was analyzed [19,33,34]. For example, Alan et al. measured the infiltration rates of 19 residential buildings by the blower door test and the tracer gas method. Since the ratio of the volume to the envelope area of the buildings was about 1:1, the correlation factor was calculated using the envelope area. As a result, the correlation factor ranged from 21 to 55, and the average value was 37 (divide-by-37 rule) [19]. To extrapolate the correlation between the fan pressurization-measured airtightness and the tracer gas-measured infiltration, it is necessary to perform the blower door test in advance. However, it is difficult to maintain a 50 Pa pressure difference between indoors and outdoors in some situations, such as large-scale or leaky buildings. While additional fans or a combination of blower door equipment and air handler units can overcome the problem, it is still difficult to maintain a 50 Pa pressure difference in reality [24,35–37]. Previous studies have used air handle units to maintain a 50 Pa pressure difference between indoors and outdoors for airtightness measurements in large-scale buildings that cannot establish a 50 Pa pressure difference [24,38]. However, there are limitations in measuring airtightness performance in large-scale buildings or buildings with numerous leakage points.

2. Methodology

2.1. Fan Pressure Method—Blower Door Test

Among various methods for airtightness measurements, the fan pressurization method employs artificial pressure conditions between indoor and outdoor fans. Figure 2 shows that the airtightness was measured using a blower door system. Specifically, the airflow rate was monitored to induce a particular pressure between the interior and exterior of the building. To set up the pressure–leakage relationship, the airflow rate passing the fans was also measured [37].

$$Q = C(\Delta p)^n \tag{1}$$

where Q [m^3/h] is the airflow rate through the opening, and C [$m^3/(h{\cdot}Pa^n)$] is the flow coefficient. In addition, n is the pressure exponent.

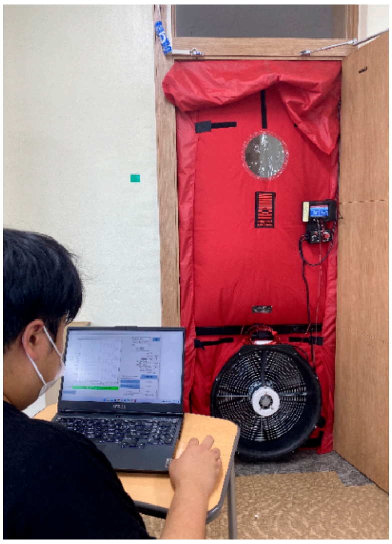

Figure 2. Blower door test.

While there are several airtightness metrics available, such as ACH_{50} (h^{-1}), ELA (m^2), EqLA (m^2), and Air permeability ($m^3/h{\cdot}m^2$), ACH_{50} was used for the present study as the metric to analyze the result obtained from the airtightness measurements. To present the metric of ACH in a natural ventilation state, it was expressed as ACH50. In addition, the blower door tests were conducted in accordance with ISO Standard 9972:2015 method 3 [39]. The windows and doors were closed for the measurements, but nothing was sealed, including the window frames and the wall.

Moreover, a blower door system was installed at the main entrance. The measurements were conducted at intervals of 5 Pa–10 Pa indoors and outdoors pressure difference by pressurizing or depressurizing from 10 Pa–65 Pa. In accordance with ISO Standard 9972, they were required that the indoor/outdoor air temperature difference should not exceed 25 °C (when the height of a building is 10 m) and the wind speed should not exceed 6 m/s. Therefore, during the Blower Door test, indoor and outdoor temperatures, humidity, and wind speed were monitored and confirmed [39].

2.2. Tracer Gas—Decay Method

The tracer gas method is one of the most highly regarded methods for infiltration measurements in buildings [40]. Three tracer gas techniques exist concentration decay, constant injection, and constant concentration [25]. Among them, the decay method is the most widespread technique for infiltration measurements due to its convenience, and compared with other techniques, it produces relatively accurate results [41–43]. While SF6 gas or CO_2 were mainly used as a tracer gas, the use of SF6 is limited due to its environmental effects [44]. Thus, CO_2 has been increasingly used [45].

For the measurement in the study, CO_2 was injected into the selected building room where the windows and doors remained closed, with the same conditions as those of the blower door method. As shown in Figure 3, the infiltration rates obtained from the decay method were calculated using Equation (2):

$$ACH = (\ln C_0 - \ln C_{(t)})/t \quad (2)$$

where C (t) is the tracer gas concentration at time (t), C_0 is the concentration of the tracer in the space at t = 0, t is time, and ACH is the air change rate (h^{-1}).

Figure 3. Tracer gas measurement.

Based on the CO_2 concentration in each room, the tracer gas was measured in the center of the room for 6 h–12 h.

2.3. Airtightness under Several Low-Pressure Differences

As a representative airtightness metric, the ACH_{50} can be calculated using Equation (3):

$$ACH_{50} = Q_{50}/V \quad (3)$$

where, Q_{50} is the air leakage rate under the 50 Pa indoor/outdoor pressure difference (m^3/h), and V is the volume (m^3).

The present study proposed a method to predict the ACH_{50} by analysing the airtightness measurements with several indoor/outdoor pressure differences of 20 Pa, 25 Pa, 30 Pa and 35 Pa. In addition, the measured values of ACH_{50} were compared with the predicted ACH_{50}. The specific methods are below:

Step 1. According to the analyses of the measured data at an interval of 5 Pa–10 Pa from 10 Pa to 65 Pa through the airtightness measurements in accordance with ISO 9972:2015, the value of ACH_{50} was compared with the measured data at several indoor/outdoor pressure differences of 20 Pa, 25 Pa, 30 Pa and 35 Pa.

Step 2. Using Equation (4), the conversion coefficient can be calculated with measured data when the value is at the ACH_{50} is assumed to be 1. For the conversion coefficient, the average values obtained from the airtightness measurements under four low-pressure differences in 6 rooms in buildings A, B, and C were used:

$$N_{pr} = ACH_{pr}/ACH_{50} \quad (4)$$

where, ACH_{50} is the air change per hour under 50 Pa (h^{-1}), and pr is the pressure difference (Pa). In addition, ACH_{pr} is the air change per hour under the various pressure differences (h^{-1}), and N_{pr} is the conversion coefficient under the various pressure differences.

Step 3. To validate the conversion coefficient, the airtightness was measured to obtain the values of ACH_{pr} (pr = 20 Pa, 25 Pa, 30 Pa and 35 Pa) in four different rooms. Moreover, the ACH_{50} was measured for the same four rooms for validation in accordance with ISO 9972:2015—method 3. The calculated ACH_{50} values (by using the measured, ACH_{pr} and Equation (4)) were compared with the measured ACH_{50} values. The difference from the comparison was identified.

The data to maintain the four pressure differences of 20 Pa, 25 Pa, 30 Pa and 35 Pa without sealing any parts in the room was measured twice. To reduce the effect of different environmental conditions, the airtightness measurement under a 50 Pa pressure difference was immediately conducted for validation.

2.4. Building Description

According to previous studies, airtightness measurements have mainly been conducted in residential buildings [10,19,46,47]. However, there have been few studies of airtightness in non-residential buildings, such as offices, schools, etc. The present study focuses on the airtightness in school buildings (Buildings A, B, and C).

Table 1 presents a description of the selected buildings. The selection of buildings was based on their building age, i.e., 1987, 1994, and 2007. The structure of all the buildings was made of reinforced concrete, and two window frames, of PVC and Aluminum, were used. In all rooms in these selected buildings, the blower door tests were performed, and both pressurization and depressurization test modes were applied twice. The tracer gas tests were also conducted in all the rooms of the selected buildings. For validation of the ACH_{pr} at 20 Pa, 25 Pa, 30 Pa, and 35 Pa, the measurements were performed in 4 rooms (A3, A4, B3, and C3).

Table 1. Building description.

	Building A				Building B			Building C		
										
Construction Year	1987				1994			2007		
Room	A1	A2	A3	A4	B1	B2	B3	C1	C2	C3
Floor plan	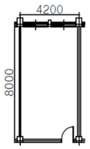	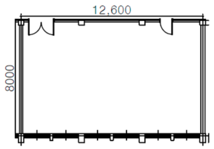	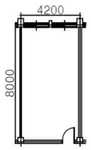	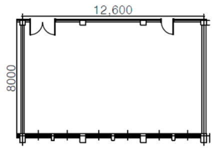	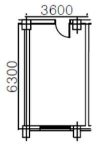	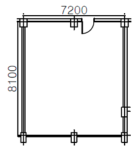	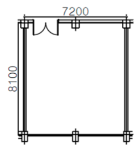	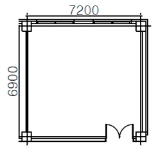	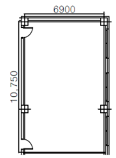	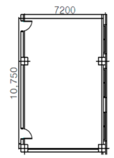
Floor area (m^2)	33.6	100.8	33.6	100.8	22.7	58.3	58.3	49.7	74.2	74.2
Volume (m^3)	90.7	272.2	90.7	272.2	51.0	157.5	157.5	134.1	200.3	200.3
Window frame	PVC	PVC	AL	AL	PVC	PVC	AL	PVC	PVC	PVC

3. Results

3.1. Blower Door Test Results

For both the fan pressurization method and tracer gas method, the indoor and outdoor temperatures were measured. The wind data were based on the weather data [48].

In Table 2, the indoor and outdoor temperatures ranged from 8.1 °C–25.1 °C and 1.9 °C–22.6 °C, respectively. The in/outdoor temperature difference ranged 0.9 °C–14.8 °C. In addition, the wind speed ranged from 0.68 m/s to 6.79 m/s, which was considered a "Moderate breeze" on the Beaufort scale of wind in ISO 9972 standard Annex D [39].

Table 2. Indoor and outdoor climate parameters during the experiment period.

Room	Measurement Date	Indoor Temp [°C]	Outdoor Temp [°C]	Indoor/Outdoor Temperature Difference [°C]	Outdoor Wind Speed [m/s]
A1	16 April 2021	22.3	14.8	7.5	1.3
	29 September 2021	24.8	22.6	2.2	3.8
A2	18 April 2021	17.0	13.4	3.6	2.6
	30 September 2021	23.1	22.2	0.9	1.0
A3	17 December 2021	17.1	2.3	14.8	6.8
	8 April 2022	16.3	10.1	6.2	1.3
A4	17 December 2021	15.0	2.7	12.3	4.5
	8 April 2022	18.7	10.1	8.6	1.5
B1	30 April 2021	20.5	18.3	2.2	3.6
	23 December 2021	16.3	4.8	11.5	4.1
B2	4 May 2021	21.5	19.3	2.2	1.7
	23 December 2021	17.4	4.8	12.6	3.6
B3	23 December 2021	16.6	4.9	11.7	3.6
C1	17 September 2021	25.1	20.9	4.2	0.7
	7 January 2022	8.1	2.4	5.7	1.7
C2	7 January 2022	8.4	1.9	6.5	1.1
	15 April 2022	20.1	14.9	5.2	3.9
C3	7 January 2022	8.7	2.2	6.5	1.9
	15 April 2022	19.0	13.2	5.8	3.9

Figure 4 shows the results of the blower door tests in two rooms in each building. Four pressurization and depressurization tests were performed in each room. As a result, the ACH_{50} values for pressurization in the room A1 were 18.50 h^{-1}–18.51 h^{-1}, while the values for depressurization were 17.42 h^{-1}–17.65 h^{-1}. The average value of ACH_{50} was 17.8 h^{-1}.

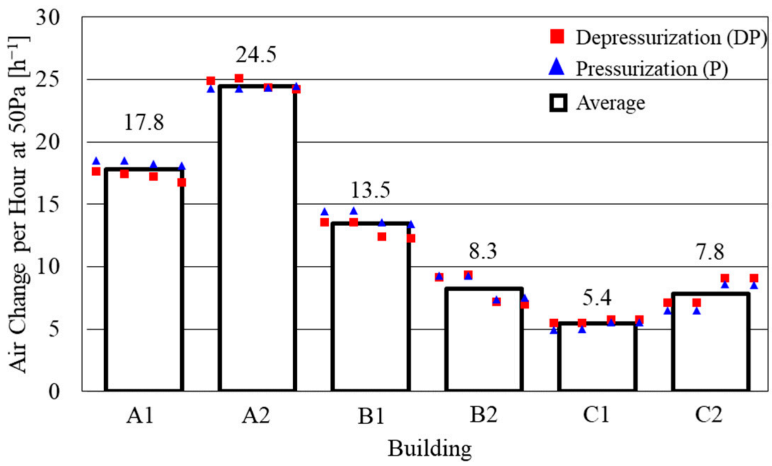

Figure 4. Airtightness performance of building rooms.

By comparing the average values of all buildings, the air leakages for buildings A, B, and C under ACH_{50} were (21.1 h^{-1}, 10.9 h^{-1} and 6.6 h^{-1}, respectively. The difference in the air leakage rates was caused by the building age [10]. Specifically, the air leakage rate of Building A, constructed in 1980, was about three times higher than that of Building C in 2000.

3.2. Tracer Gas Results and Distribution of the Correlation Factor

Figure 5 shows the measurement results obtained from the decay method.

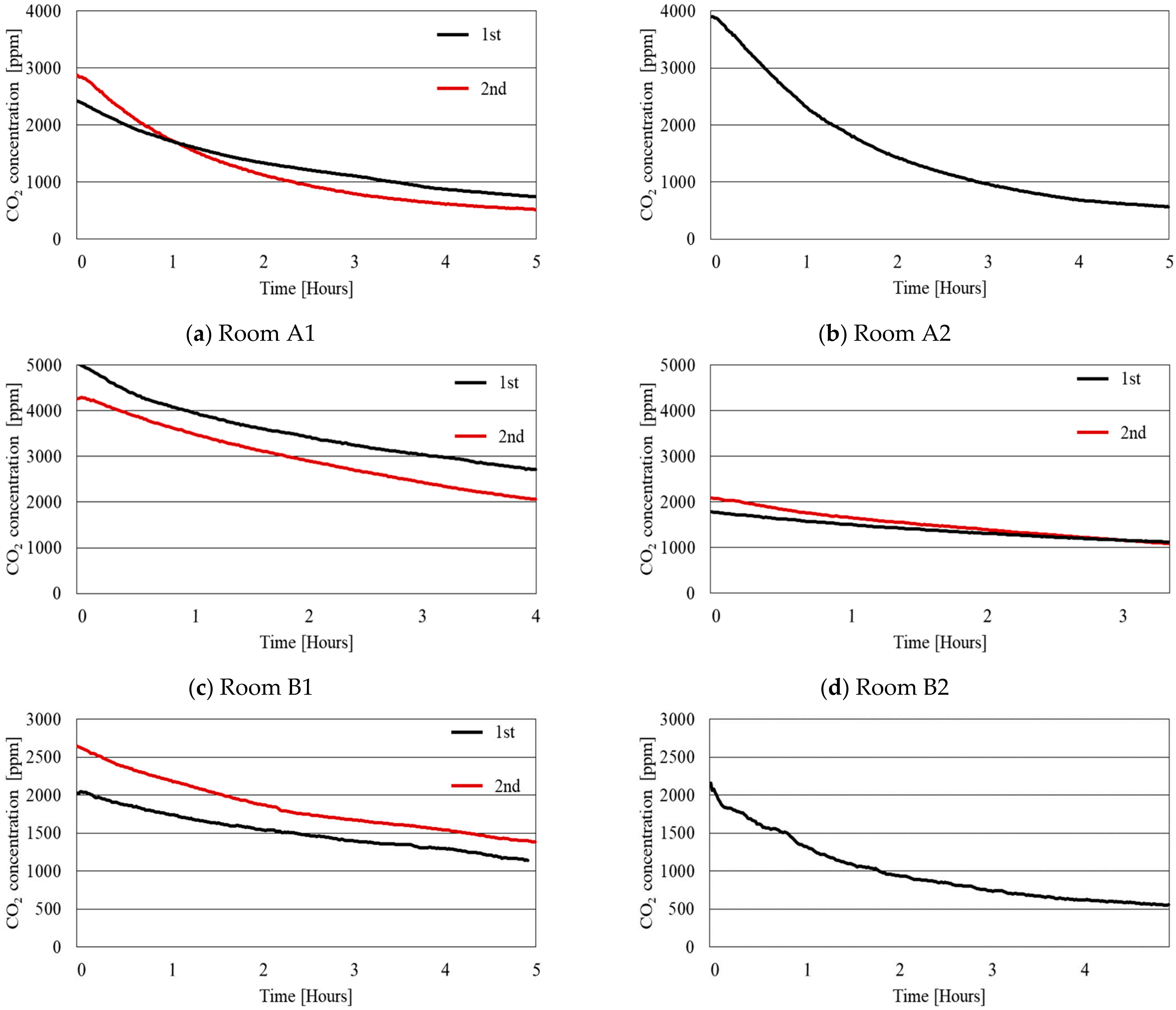

(**a**) Room A1 (**b**) Room A2 (**c**) Room B1 (**d**) Room B2 (**e**) Room C1 (**f**) Room C2

Figure 5. Concentration of the rooms through tracer gas measurement.

According to the result of the decay method, the averaging infiltration rates for buildings A, B, and C were 0.3 h^{-1}, 0.16 h^{-1} and 0.09 h^{-1}, respectively. Similarly, the lowest infiltration rate was observed in building C, as with the blower door test results. The averaging infiltration rates of building A were about three times higher than that of building C due to the blower door method.

Table 3 shows the infiltration rates obtained from the decay method and the blower door test that were analyzed to determine the distribution of the correlation factors in non-residential buildings in Republic of Korea.

Table 3 presents measurement results and the correlation factors. In Table 3, the infiltration rates for room A1 were 0.22 h^{-1} and 0.29 h^{-1}, while the values under the ACH_{50} from the blower door test were 18.02 h^{-1} and 17.57 h^{-1}, respectively. In addition, the calculated correlation factor was 81.91 based on the measurement results obtained from the blower door test and the decay method.

Table 3. Airtightness performance measurement results and distribution of the correlation factor.

Room	Air Change per Hour (h^{-1}, ACH) Using the Decay Method	Air Change per Hour at 50 Pa (ACH_{50}) Using the Blower Door Test	ACH_{50}/ACH
A1	0.22	18.02	81.91
	0.29	17.57	60.58
A2	0.21	24.64	117.31
B1	0.16	14.02	87.59
	0.15	12.91	86.08
B2	0.15	9.26	61.73
	0.18	7.25	40.29
C1	0.09	5.21	57.83
	0.09	5.64	62.64
C2	0.09	6.79	75.42

When estimating the correlation factors based on the measurement results of the blower door test and the decay method, the factors ranged from 40.29−117.31. The average correlation factor was 73.14, about 3.6 times higher than that suggested by Sherman (divided-by-20 rule). Alan et al. estimated the distribution of correlation factors through the comparison between the measurement of air permeability ($m^3/h{\cdot}m^2$) and the results of the tracer gas method in residential buildings in the UK [19]. As a result, the factors were distributed in the range of 20.54−55.06, and the average value was 36.53.

Comparing the averaging correlation factors of each building, the values for buildings A, B, and C were 86.6, 68.93, and 65.3, respectively. The highest correlation factor can be caused by the highest air leakage rates in a building.

4. Results ACH of Several Low-Pressure Differences

In this study, the air leakage rates under several pressure differences (ACH_{pr}, pr = 20 Pa, 25 Pa, 30 Pa, 35 Pa and 50 Pa) and Equation (4) for the calculation of N_{pr} were analyzed. Equation (4) was used to convert the data obtained from the blower door test in the selected buildings into ACH_{50} values. In addition, the value of conversion coefficients was calculated.

In this chapter, the ACH_{pr} was measured in rooms A3, A4, B3, and C3 in the selected buildings. The conversion coefficients (N_{pr}) were calculated through comparison with the measured ACH_{50} values.

${ACH_{50}}^P$ was predicted based on the conversion coefficients and the measured ACH_{pr} values using Equation (5):

$$ACH_{pr}/N_{pr} = {ACH_{50}}^P \quad (5)$$

where, pr = 20 Pa, 25 Pa, 30 Pa and 35 Pa.

Figure 6 shows the distribution of the conversion coefficients obtained from the blower door test, which were calculated under four low-pressure differences of 20 Pa, 25 Pa, 30 Pa and 35 Pa, assuming that the ACH_{50} was 1.

The distribution of the conversion coefficients under the 20 Pa indoor and outdoor pressure difference was from 0.55 to 0.73, in which the average value was 0.60. For this study, the average conversion coefficient was used, and the values of ACH_{pr} 20 Pa, 25 Pa, 30 Pa and 35 Pa were 0.60, 0.68, 0.76, and 0.84, respectively. Figure 7 presents the results obtained to verify the conversion coefficient in Room A3. To validate this, the airtightness performance (ACH 20, ACH 25, ACH 30, ACH 35) at the corresponding pressure differences was divided by the conversion coefficient (20 Pa = 0.60, 25 Pa = 0.68, 30 Pa = 0.76, 35 Pa = 0.84) presented in Figure 6 to calculate ACH 50. According to the result obtained in room A3, the depressurization and pressurization values under ACH_{20} were 8.2 h^{-1} and 9.2 h^{-1}, respectively, as shown in Figure 7. Moreover, the same measurements under the pressure differences of 25 Pa, 30 Pa and 35 Pa were performed in rooms A4, B3, and C3.

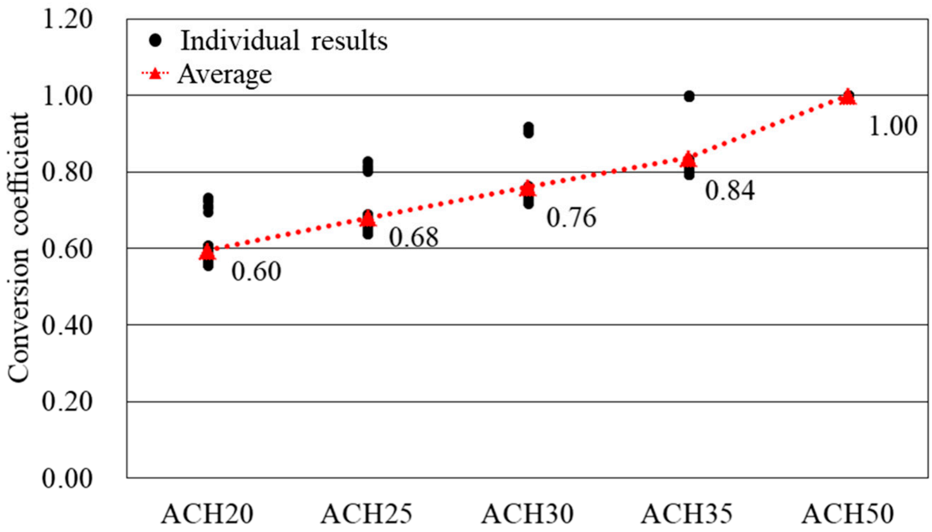

Figure 6. Distribution of conversion coefficients at several pressure differences.

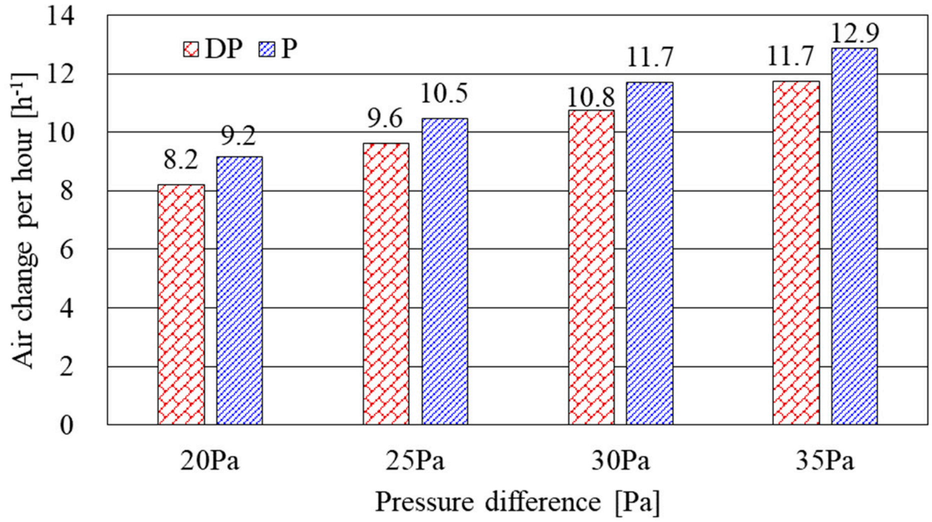

Figure 7. ACHpr under four low-pressure differences in room A3.

The values of $ACH_{50}{}^{P}$ can be calculated using Equation (5). The values of $ACH_{50}{}^{P}$ were compared with the values of $ACH_{50}{}^{M}$ for validation, which was obtained from the measurements in the rooms in accordance with ISO 9972: Method 3. Figure 8 presents the values of $ACH_{50}{}^{P}$ and $ACH_{50}{}^{M}$. To calculate the values of $ACH_{50}{}^{P}$, the measured data under the 20 Pa pressure difference was divided by the conversion coefficient 0.60 in Figure 6. As a result, the $ACH_{50}{}^{P}(ACH_{20}/N_{20})$ was 14.6 h^{-1}, while the $ACH_{50}{}^{M}$ obtained from the measurement in the same room was 15.2 h^{-1}. The difference between these values was 4.4%. By comparing the difference between $ACH_{50}{}^{M}$ and $ACH_{50}{}^{P}$ in Table 4, the results are 3–4.4%, 0.1–4.4% and 0.4–2.9% for buildings A, B, and C, respectively. For comparison under the indicated pressure differences in Table 4, they were 0.7–4.4%, 1.0–3.2%, 0.1–3.1% and 0.9–4.1% for ACH_{20}, ACH_{25}, ACH_{30}, and ACH_{35}, respectively.

A comparison of the values under several pressure differences shows that the results are evenly distributed. In addition, the conversion coefficients are evenly distributed and seem not to be affected by the building age. Therefore, it is shown that the conversion coefficients can be used to convert the measured data under a lower pressure difference than 50 Pa in the building where large air leakages occur or which has a large volume into ACH_{50} values.

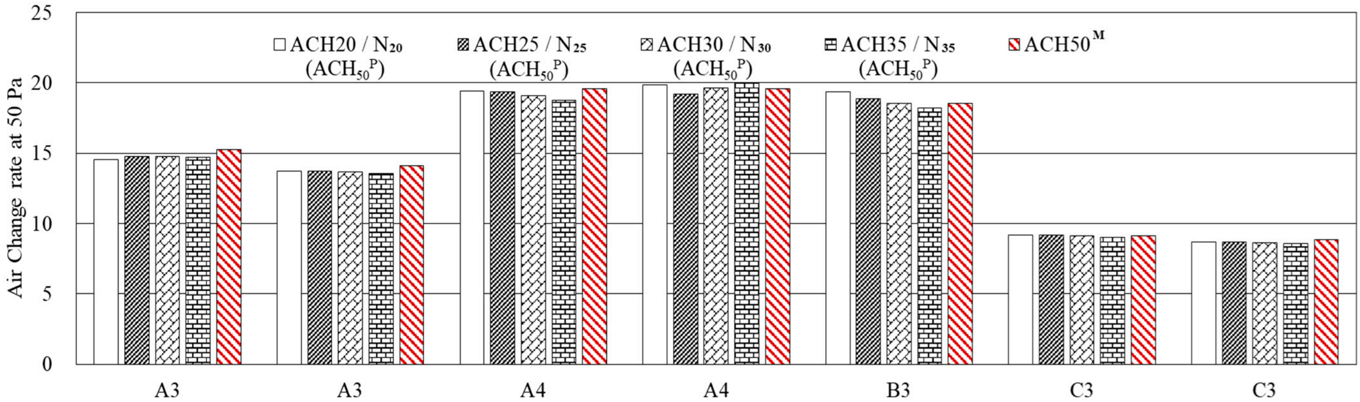

Figure 8. Comparison of ACH_{pr} divided by conversion coefficient with measurement ACH_{50}.

Table 4. Results of ACH_{pr} divided by N_{pr} and errors.

	$ACH_{50}{}^{M}$	ACH_{20}/N_{20} ($ACH_{50}{}^{P}$)	Error (%)	ACH_{25}/N_{25} ($ACH_{50}{}^{P}$)	Error (%)	ACH_{30}/N_{30} ($ACH_{50}{}^{P}$)	Error (%)	ACH_{35}/N_{35} ($ACH_{50}{}^{P}$)	Error (%)
A3	15.2	14.6	4.4	14.8	3.2	14.8	3.1	14.8	3.1
	14.1	13.7	2.5	13.7	2.8	13.6	3.2	13.6	3.2
A4	19.6	19.4	0.8	19.3	1.2	19.1	2.4	19.1	2.4
	19.6	19.8	1.3	19.2	2.1	19.6	0.3	19.6	0.3
B3	18.5	19.3	4.4	18.9	1.9	18.5	0.1	18.5	0.1
C3	9.1	9.2	0.7	9.2	1.0	9.1	0.4	9.1	0.4
	8.9	8.7	2.1	8.7	1.8	8.6	2.3	8.6	2.3

5. Discussion and Conclusions

The present study identified the airtightness and distribution of the correlation factors for non-residential buildings in Republic of Korea. In addition, the study also proposed a method to calculate the airtightness under the low-pressure difference caused by large air leakage in the building or large building volume.

The distribution of the values of ACH_{50} obtained from the blower door test in non-residential buildings in Republic of Korea increased according to the increase in building age. The average values in two rooms in buildings A and C, built in 1987 and 2007, were 21.1 h^{-1} and 6.6 h^{-1}, respectively. The air leakage rates in Building A were about three times higher than in Building C.

The correlation factors through the comparison of the results obtained from the blower door test and the tracer gas method ranged from 40.29 to 117.31. A comparison of these values with the factor (N = 20, dived-by-20 rule) proposed by Sherman showed the high difference between them. In addition, they also showed a high difference compared with the value of 36.53 determined by Alan et al. Specifically, the correlation factors for buildings A, B, and C were 86.60, 68.93, and 65.30, respectively. In this study, it was difficult to determine the value of the correlation factor properly. There was a limit in that the value was larger than other studies. Further, determining the representative correlation factor for various buildings is necessary, considering the construction year, WWR (window-to-wall ratio), locations, etc.

The conversion coefficient N_{pr} was proposed to convert values under low-pressure differences of 20 Pa, 25 Pa, 30 Pa and 35 Pa into the ACH_{50} value. To verify the conversion coefficient, the measurements under low-pressure differences of 20 Pa, 25 Pa, 30 Pa and 35 Pa were performed. The values of $ACH_{50}{}^{P}$ were calculated using the conversion coefficient (N_{pr}). As a result, the differences between the $ACH_{50}{}^{P}$ and the $ACH_{50}{}^{M}$ values were less than 5%.

In the future, it is necessary to investigate the accuracy of conversion coefficients through measurements for residential buildings and buildings with various purposes. In addition, a study will be conducted to confirm the possibility of measurement at a lower pressure difference. This will be achieved by calculating the conversion coefficient based on measurement results at a pressure difference lower than 20 Pa and comparing it with ACH50 measurement results.

Author Contributions: Conceptualization, G.H.; Methodology, C.S.; Data curation, C.S.; Writing—original draft, C.S.; Writing—review & editing G.H.; Visualization, C.S.; Supervision, G.H.; Funding acquisition, G.H. All authors have read and agreed to the published version of the manuscript.

Funding: This study was supported by a 2021 Research Grant from Kangwon National University and the National Research Foundation of Korea (NRF) grant funded by the Korean government (MSIT) (NRF-2020R1C1C1010801).

Data Availability Statement: The data presented in this study are available on request from the first author. Data sharing is not applicable.

Conflicts of Interest: The authors declare no conflict of interest.

References

1. Jones, B.; Das, P.; Chalabi, Z.; Davies, M.; Hamilton, I.; Lowe, R.; Mavrogianni, A.; Robinson, D.; Taylor, J. Assessing Uncertainty in Housing Stock Infiltration Rates Andassociated Heat Loss: English and UK Case Studies. *Build. Environ.* **2015**, *92*, 644–656. [CrossRef]
2. Al-Sakkaf, A.; Bagchi, A.; Zayed, T. Evaluating Life-Cycle Energy Costs of Heritage Buildings. *Buildings* **2022**, *12*, 1271. [CrossRef]
3. Economidou, M.; Todeschi, V.; Bertoldi, P.; D'Agostino, D.; Zangheri, P.; Castellazzi, L. Review of 50 years of EU Energy Efficiency Policies for Buildings. *Energy Build.* **2020**, *225*, 110322. [CrossRef]
4. Lapillonne, B.; Pollier, K.; Samci, N. Energy Efficiency Trends for Households in the EU. *Enerdata* **2014**, *22*, 2015.
5. Li, T.; Xia, J.; Chin, C.S.; Song, P. Investigation of the Thermal Performance of Lightweight Assembled Exterior Wall Panel (LAEWP) with Stud Connections. *Buildings* **2022**, *12*, 473. [CrossRef]
6. Lee, J.; Kim, J.; Song, D.; Kim, J.; Jang, C. Impact of External Insulation and Internal Thermal Density upon Energy Consumption of Buildings in a Temperate Climate with Four Distinct Seasons. *Renew. Sustain. Energy Rev.* **2017**, *75*, 1081–1088. [CrossRef]
7. Korea Energy Agency (KEA). *Commentaries for Building Energy Code*; Korea Energy Agency (KEA): Ulsan, Republic of Korea, 2018.
8. Shim, C.; Seong, N.; Hong, G. An Analysis of ACHn for Improving the Performance of Green Remodeling through the Airtightness Measurements. *KIEAE J.* **2021**, *21*, 7–12. [CrossRef]
9. Poza-Casado, I.; Meiss, A.; Padilla-Marcos, M.Á.; Feijó-Muñoz, J. Airtightness and Energy Impact of Air Infiltration in Residential Buildings in Spain. *Int. J. Vent.* **2021**, *20*, 258–264. [CrossRef]
10. Hong, G.; Kim, C. Experimental Analysis of Airtightness Performance in High-Rise Residential Buildings for Improved Code-Compliant Simulations. *Energy Build.* **2022**, *261*, 111980. [CrossRef]
11. Erhorn-Kluttig, H.; Erhorn, H.; Lahmidi, H. Airtightness Requirements for High Performance Building Envelopes. *EPBD Build. Platf.* **2009**, *157*, 1–6.
12. Etheridge, D. A Perspective on Fifty Years of Natural Ventilation Research. *Build. Environ.* **2015**, *91*, 51–60. [CrossRef]
13. Miszczuk, A. Influence of Air Tightness of the Building on Its Energy-Efficiency in Single-Family Buildings in Poland. In *MATEC Web of Conferences*; EDP Sciences: Les Ulis, France, 2017; Volume 117. [CrossRef]
14. Jing, J.; Lee, D.S.; Joe, J.; Kim, E.J.; Cho, Y.H.; Jo, J.H. A Sensing-Based Visualization Method for Representing Pressure Distribution in a Multi-Zone Building by Floor. *Sensors* **2023**, *23*, 4116. [CrossRef] [PubMed]
15. Kravchenko, I.; Kosonen, R.; Jokisalo, J.; Kilpeläinen, S. Performance of Modern Passive Stack Ventilation in a Retrofitted Nordic Apartment Building. *Buildings* **2022**, *12*, 96. [CrossRef]
16. Ji, Y.; Duanmu, L. Airtightness Field Tests of Residential Buildings in Dalian, China. *Build. Environ.* **2017**, *119*, 20–30. [CrossRef]
17. Vinha, J.; Manelius, E.; Korpi, M.; Salminen, K.; Kurnitski, J.; Kiviste, M.; Laukkarinen, A. Airtightness of Residential Buildings in Finland. *Build. Environ.* **2015**, *93*, 128–140. [CrossRef]
18. Miszczuk, A.; Heim, D. Parametric Study of Air Infiltration in Residential Buildings—The Effect of Local Conditions on Energy Demand. *Energies* **2021**, *14*, 127. [CrossRef]
19. Pasos, A.V.; Zheng, X.; Smith, L.; Wood, C. Estimation of the Infiltration Rate of UK Homes with the Divide-by-20 Rule and Its Comparison with Site Measurements. *Build. Environ.* **2020**, *185*, 107275. [CrossRef]
20. Hong, G.; Kim, D.D. Airtightness of Electrical, Mechanical and Architectural Components in South Korean Apartment Buildings Using the Fan Pressurization and Tracer Gas Method. *Build. Environ.* **2018**, *132*, 21–29. [CrossRef]
21. Cheong, K.W. Airflow Measurements for Balancing of Air Distribution Systems—Tracer-Gas Technique as an Alternative? *Build. Environ.* **2001**, *36*, 955–964. [CrossRef]
22. Goubran, S.; Qi, D.; Saleh, W.F.; Wang, L. Comparing Methods of Modeling Air Infiltration through Building Entrances and Their Impact on Building Energy Simulations. *Energy Build.* **2017**, *138*, 579–590. [CrossRef]

23. Martín-Garín, A.; Millán-García, J.A.; Hidalgo-Betanzos, J.M.; Hernández-Minguillón, R.J.; Baïri, A. Airtightness Analysis of the Built Heritage field Measurements of Nineteenth Century Buildings through Blower Door Tests. *Energies* **2020**, *13*, 6726. [CrossRef]
24. Kim, M.H.; Jo, J.H.; Jeong, J.W. Feasibility of Building Envelope Air Leakage Measurement Using Combination of Air-Handler and Blower Door. *Energy Build.* **2013**, *62*, 436–441. [CrossRef]
25. Resources, R.C. F16 SI: Ventilation and Infiltration. In *Ashrae Handbook*; ASHRAE: Norfolk, VA, USA, 2009.
26. Li, X.; Zhou, W.; Duanmu, L. Research on Air Infiltration Predictive Models for Residential Building at Different Pressure. *Build. Simul.* **2021**, *14*, 737–748. [CrossRef]
27. Sherman, M.H. Tracer-Gas Techniques for Measuring Ventilation in a Single Zone. *Build. Environ.* **1990**, *25*, 365–374. [CrossRef]
28. Lee, D.S.; Jeong, J.W.; Jo, J.H. Experimental Study on Airtightness Test Methods in Large Buildings; Proposal of Averaging Pressure Difference Method. *Build. Environ.* **2017**, *122*, 61–71. [CrossRef]
29. Cui, S.; Cohen, M.; Stabat, P.; Marchio, D. CO_2 Tracer Gas Concentration Decay Method for Measuring Air Change Rate. *Build. Environ.* **2015**, *84*, 162–169. [CrossRef]
30. Sherman, M.H.; Dickerhoff, D.J. Airtightness of U.S. Dwellings. *ASHRAE Trans.* **1998**, *104*, 1359–1367.
31. Sherman, M.H. Estimation of Infiltration from Leakage and Climate Indicators. *Energy Build.* **1987**, *10*, 81–86. [CrossRef]
32. Lutzkendorf, T.; Balouktsi, M. *Energy Conservation in Buildings and Community Systems Programme*; IEA: Paris, France, 2016; pp. 35–42, Annex 57; Available online: http://www.annex57.org/wp/wp-content/uploads/2017/05/ST2_Repor.pdf (accessed on 5 October 2022).
33. Kang, K.; Lee, S.-W.; Lee, E.-J.; Park, M.-J.; Lim, J.-H.; Jo, B.-R.; Lee, J.-C. Infiltration : Just ACH50 Divided by 20? Concentrated on a Residential Building. *SAREK Summer Conf.* **2015**, *6*, 435–439.
34. Hyon, M.J.; Ik, L.J.; Sung, K.M. Study on Estimation of Infiltration Rate (ACH Natural) Using Blower Door Test Results. *J. KIAEBS* **2020**, *14*, 687–698.
35. Erin, L.; Max, H. *Blower-Door Techniques for Measuring Interzonal Leakage: A Preliminary Report*; Ernest Orlando Lawrence Berkeley National Laboratory: Berkeley, CA, USA, 2013.
36. Bahnfleth, W.P.; Yuill, G.K.; Lee, B.W. Protocol for Field Testing of Tall Buildings to Determine Envelope Air Leakage Rate. *ASHRAE Trans.* **1999**, *105*, 27.
37. Zheng, X.; Cooper, E.; Gillott, M.; Wood, C. A Practical Review of Alternatives to the Steady Pressurisation Method for Determining Building Airtightness. *Renew. Sustain. Energy Rev.* **2020**, *132*, 110049. [CrossRef] [PubMed]
38. Jeong, J.W.; Firrantello, J.; Bahnfleth, W.P.; Freihaut, J.D.; Musser, A. Case Studies of Building Envelope Leakage Measurement Using an Air-Handler Fan Pressurisation Approach. *Build. Serv. Eng. Res. Technol.* **2008**, *29*, 137–155. [CrossRef]
39. *EN ISO 9972:2015*; Thermal Performance of Buildings—Determination of Air Permeability of Buildings—Fan Pressurization Method. Standards Australia: Sydney, Australia, 2015.
40. Frattolillo, A.; Stabile, L.; Dell'Isola, M. Natural Ventilation Measurements in a Multi-Room Dwelling: Critical Aspects and Comparability of Pressurization and Tracer Gas Decay Tests. *J. Build. Eng.* **2021**, *42*, 102478. [CrossRef]
41. Lo, L.J.; Novoselac, A. Cross Ventilation with Small Openings: Measurements in a Multi-Zone Test Building. *Build. Environ.* **2012**, *57*, 377–386. [CrossRef]
42. Nikolopoulos, N.; Nikolopoulos, A.; Larsen, T.S.; Nikas, K.S.P. Experimental and Numerical Investigation of the Tracer Gas Methodology in the Case of a Naturally Cross-Ventilated Building. *Build. Environ.* **2012**, *56*, 379–388. [CrossRef]
43. Jankovic, A.; Gennaro, G.; Chaudhary, G.; Goia, F.; Favoino, F. Tracer Gas Techniques for Airflow Characterization in Double Skin Facades. *Build. Environ.* **2022**, *212*, 108803. [CrossRef]
44. Almeida, R.M.S.F.; Barreira, E.; Moreira, P. A Discussion Regarding the Measurement of Ventilation Rates Using Tracer Gas and Decay Technique. *Infrastructures* **2020**, *5*, 85. [CrossRef]
45. Batterman, S. Review and Extension of CO2-Based Methods to Determine Ventilation Rates with Application to School Classrooms. *Int. J. Environ. Res. Public Health* **2017**, *14*, 145. [CrossRef]
46. Sinnott, D. Dwelling Airtightness: A Socio-Technical Evaluation in an Irish Context. *Build. Environ.* **2016**, *95*, 264–271. [CrossRef]
47. Shin, H.K.; Jo, J.H. Air Leakage Characteristics and Leakage Distribution of Dwellings in High-Rise Residential Buildings in Korea. *J. Asian Archit. Build. Eng.* **2013**, *12*, 87–92. [CrossRef]
48. KMA, Daily Data, (2021–2022). Available online: https://Www.Weather.Go.Kr/w/Obs-Climate/Land/Past-Obs/Obs-by-Day.Do (accessed on 5 October 2022).